

# Observation of asymmetric Bloch walls in epitaxial Co films with strong in-plane uniaxial anisotropy

I. L. Prejbeanu, L. D. Buda, U. Ebels, and K. Ounadjela<sup>a)</sup>

*Institut de Physique et Chimie des Matériaux de Strasbourg, CNRS (UMR 7504), 23 rue du Loess, 67037 Strasbourg Cedex, France*

(Received 12 May 2000; accepted for publication 11 September 2000)

Combined studies involving magnetic force microscopy and micromagnetic simulations are used to investigate the domain wall structure in epitaxial Co(10 $\bar{1}$ 0) thin films with strong in-plane uniaxial magneto-crystalline anisotropy. This letter shows experimental evidence that, for such a system, the domain wall structure transforms from an asymmetric Bloch wall into an asymmetric Néel wall upon decreasing the film thickness from 100 to 20 nm. This transition occurs without cross-tie wall formation. Furthermore, it is found that from the four possible energetically equivalent asymmetric Bloch wall configurations, only two are stabilized along a single domain wall. For a given wall, the transition from one configuration to the other involves the simultaneous reversal of the polarity of the Bloch core and the Néel cap. © 2000 American Institute of Physics.

[S0003-6951(00)03045-X]

The application of small magnetic elements in high density data storage requires a detailed understanding of their magnetic microstructure. For in-plane magnetized thin films, the spin configuration of domain walls has a two dimensional structure due to the magneto-static stray fields at the film surfaces.<sup>1-3</sup> The details of the wall configurations are strongly dependent on the film thickness as well as on the ratio,  $Q$ , between the anisotropy energy  $K_u$  and the demagnetization energy  $2\pi M_s^2$  ( $Q = K_u/2\pi M_s^2$ ). Many experimental as well as numerical studies have been performed for soft magnetic materials<sup>4-7</sup> such as Permalloy ( $Q \approx 2.5 \times 10^{-4}$ ). For very thick films the wall is dominantly Bloch-like in the film center and terminated by Néel caps at the film surface. Upon reducing the thickness, this wall turns into an asymmetric Bloch wall (vortex wall), then into a complex cross-tie wall and finally for very thin films into a symmetric Néel wall.<sup>4</sup> Cross-tie walls are modified Néel walls, in which the 180° wall transitions are partially replaced by energetically more favorable 90° transitions. This results in a deviation of the magnetization from the easy axis inside the domains. The increase of the anisotropy energy due to this deformation is negligible for low- $Q$  materials. This will not be the case for materials in which the anisotropy energy is comparable to the demagnetization energy.

Not many experimental studies exist for materials having a strong in-plane uniaxial anisotropy comparable to the demagnetization energy, leading to a moderate  $Q$  factor close to, but still smaller than one.<sup>8</sup> In this letter, it is shown experimentally that for epitaxial Co(10 $\bar{1}$ 0) thin films with  $Q = 0.4$  the domain wall structure transforms from an asymmetric Bloch wall into an asymmetric Néel wall upon decreasing the film thickness. In contrast to soft magnetic materials, this transition occurs for the Co films at much lower thicknesses, since it is determined by the Bloch wall width parameter. The enhanced anisotropy, which leads to a smaller domain wall width, scales this transition from Bloch

to Néel wall and prevents the formation of cross-tie walls.

The epitaxial Co films were grown by e-beam evaporation under ultrahigh vacuum conditions. An initial 20 nm bcc Cr(211) buffer layer was deposited at 400 °C directly on an MgO(110) substrate allowing to stabilize the (10 $\bar{1}$ 0) hcp structure of the Co layer with the  $c$  axis in the film plane. The Co layer itself was deposited at the same temperature on top of the Cr buffer and was capped with a 4-nm-thick Pt layer (deposited at room temperature) to prevent oxidation. The crystal quality was confirmed by *in situ* reflection high energy electron diffraction and *ex situ* x-ray diffraction measurements, indicating a very low spread of the in-plane  $c$  axis of the hcp Co films.<sup>9</sup> From magnetometric measurements the magneto-crystalline anisotropy was determined ( $K_u = 4.8 \pm 0.3 \times 10^6$  erg/cm<sup>3</sup>). The homogeneity of the films are furthermore confirmed by hysteresis loop measurements. For fields applied along the easy axis, the hysteresis loops are square having a low coercivity (50–400 Oe) compared to the anisotropy field (8–9 kOe). This indicates that the reversal is governed by a domain wall nucleation and propagation process. It is noted that the coercive field increases with decreasing film thickness and correlates with the wall energy deduced from micromagnetic calculations.

In order to deduce the spin configuration of the domain wall as a function of film thickness, numerical simulations were performed. These calculations are based on the two dimensional LaBonte method<sup>1</sup> in which the continuous magnetization distribution is discretized into infinite prisms with uniform magnetization, see Fig. 1(a). These prisms have a square cross section with a lattice constant of 2 nm, smaller than the exchange parameter ( $l_{ex} = \sqrt{A_{ex}/(2\pi M_s^2)}$  for Co is 3.37 nm). The total free energy of the domain wall is evaluated taking into account the magneto-crystalline anisotropy, the exchange energy and the stray field energy from which the total local effective field  $\mathbf{H}_{eff}$  is evaluated.<sup>1-3</sup> The Landau-Lifshitz-Gilbert equation

<sup>a)</sup>Electronic mail: kamel@ipcms.u-strasbg.fr

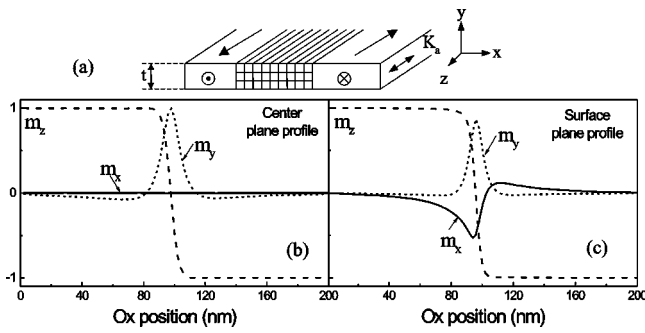


FIG. 1. A schematic showing the coordinate system and the geometry of the discretization scheme (a). The line profiles of all three magnetization components taken perpendicular to the wall along the center plane (b) and the surface plane (c). The material parameters used in the simulation are: exchange constant  $A_{ex} = 1.4 \times 10^{-6}$  erg/cm, anisotropy constant  $K_u = 5 \times 10^6$  erg/cm<sup>3</sup> and saturation magnetization  $M_s = 1400$  emu/cm<sup>3</sup>.

$$(1 + \alpha^2) \frac{\partial \mathbf{m}}{\partial t} = -\gamma \mathbf{m} \times \mathbf{H}_{eff} - \alpha \gamma \mathbf{m} \times [\mathbf{m} \times \mathbf{H}_{eff}] \quad (1)$$

is integrated numerically by an explicit scheme under the constraint of  $|\mathbf{m}(\mathbf{r}, t)|^2 = 1$  and using a time step of 0.1 ps. The term  $\gamma$  is the gyromagnetic ratio and  $\alpha$  is the damping parameter which is settled to 1.0. It was found that the value of  $\alpha$  does not alter the final stable magnetization state.<sup>10</sup> The equilibrium domain wall configuration is reached when the largest residual value of the normalized torque  $|\mathbf{m} \times \mathbf{H}_{eff}| / (4\pi M_s)$  is less than  $10^{-6}$ . The stability of each solution is checked by slightly perturbing the final state with a random magnetization fluctuation. For the stable solutions obtained the self-consistency parameter  $S$ , defined by Aharoni,<sup>11</sup> differs from unity by 0.01%.

Typical line profiles perpendicular to the wall are shown in Figs. 1(b) and 1(c) for all three magnetization components taken along the center plane as well as along the surface plane (the film thickness is 100 nm). For this thickness, the domain walls in the film center are dominantly Bloch-like, expressed by the fact that the  $m_x$  component of the magnetization remains zero [Fig. 1(b), full line]. This Bloch part is terminated by an asymmetric Néel cap at the film surface, expressed by the nonzero  $m_x$  component [Fig. 1(c), full line]. However, the  $m_y$  component at the film surface does not vanish, which means that the Néel cap retains some Bloch character. Hence, a complete flux closure such as in FeNi films does not develop which is due to the stronger uniaxial anisotropy in the Co(10 $\bar{1}$ 0) films.

The calculated two dimensional spin configuration inside the domain walls is shown in more detail for three different thicknesses in Fig. 2(a):  $t = 100, 50$ , and  $20$  nm. The configuration of the  $50$  nm wall is qualitatively the same as the one of the  $100$  nm wall, with a dominant Bloch wall of reduced length and an asymmetric Néel cap at the surface. For these walls two configurations exist, an “S” shape and a “C” shape as indicated in the schematic of Fig. 2(a). For  $20$ -nm-thick films the S shape configuration is stabilized, corresponding to an asymmetric Néel wall. In this case, the vortex of the C shape would increase the exchange energy above the gain in demagnetizing energy. In contrast, for thicknesses above  $20$  nm a C shape configuration is favored which corresponds to an asymmetric Bloch wall.

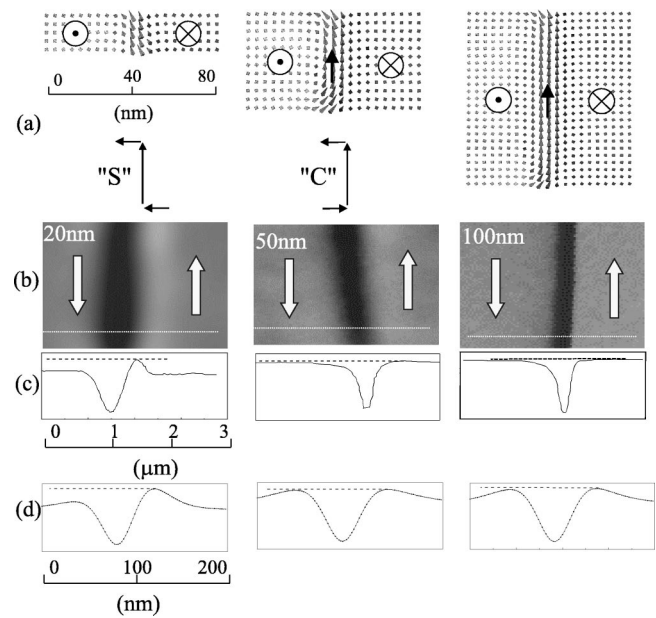


FIG. 2. (a) The calculated spin configuration of the domain walls in Co(10 $\bar{1}$ 0) thin films for  $t = 20, 50, 100$  nm. The two configurations denoted by S and C are schematically sketched. (b) The MFM images corresponding to the same thickness as in (a). The walls were induced after saturating in a field perpendicular to the film plane. (c) The corresponding experimental line profiles of the image contrast taken along a line perpendicular to the wall as indicated in (b). (d) The simulated line profile calculated from the interaction between a pyramidal tip and the stray fields corresponding to the magnetic configurations shown in (a). To take into account the convolution effect, a large number of 20 planes was chosen to model the pyramidal tip (see Ref. 12).

Magnetic force microscope (MFM) images of the domain walls for these three thicknesses are shown in Fig. 2(b). The walls appear as dominantly black lines between antiparallel “gray” domains. Since MFM is sensitive to the stray fields emanating from the sample surface, the magnetization distribution inside the sample cannot be directly deduced. However, the asymmetric domain walls studied here contain a Bloch core in the film center and a Néel surface cap which each have a characteristic charge distribution generating a specific stray field distribution sensed by the MFM tip. In particular, for all three thicknesses the interaction with the Bloch part dominates, giving rise to a strong symmetric contrast. In our case, white contrast denotes repulsive interaction for Bloch walls pointing upwards and black contrast denotes attractive interaction for Bloch walls pointing downwards. In contrast, the stray fields from the Néel cap give rise to a black–white double contrast, indicating its rotation sense. For the  $100$ -nm-thick film, with a pronounced Bloch core, the experimental line profile shown in Fig. 2(c) is almost symmetric, with a slight asymmetry. This asymmetry increases with decreasing film thickness, due to the decrease of the Bloch core fraction. The asymmetry is very pronounced for the  $20$ -nm-thick Co film showing a white border adjacent to the black Bloch part. This double contrast indicates the formation of an asymmetric Néel wall.

In order to compare the measured line profiles of the domain walls shown in Fig. 2(c) with the calculated spin configuration shown in Fig. 2(a), the MFM response was modeled. It is noted that the MFM used was equipped with CoCr coated Si cantilevers of pyramidal shape, magnetized

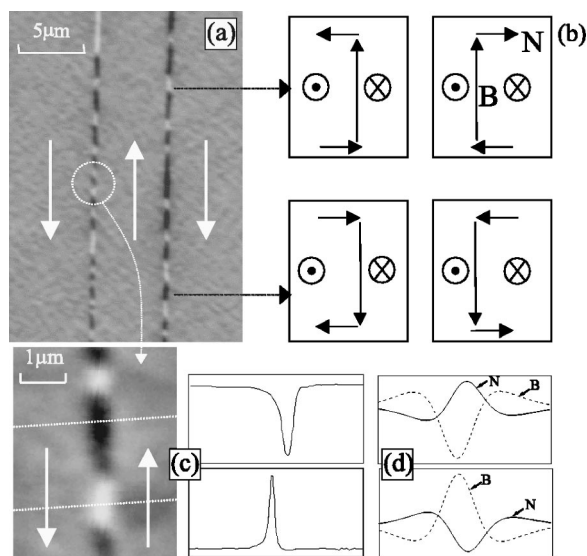


FIG. 3. (a) The MFM image of a 50-nm-thick Co film after perpendicular demagnetization. The domain walls contain segments of alternating black and white contrasts. These indicate opposing Bloch core orientations. The four possible Bloch core and Néel cap polarities are sketched in (b). (c) A zoom of the alternating wall contrasts and the corresponding line profiles. The sign as well as the asymmetry of the line profile change upon transition from a black to a white segment. (d) The deconvolution of the simulated asymmetric line profiles shows the Bloch contribution (B) and the Néel contribution (N) to the contrast.

along the tip axis. The simulated line profile was obtained by computing the magnetic force gradient generated by the spin configuration of the wall.<sup>12,13</sup> The results are shown in Fig. 2(d) and reproduce qualitatively the experimental line shapes, but not quantitatively the wall width. The convolution effect from the pyramidal tip shape with the long range dipolar stray fields produced by the domain walls does not allow a quantitative analysis of the experimental line profile. This convolution can be simulated by varying the tip shape between a single dipole tip and a pyramidal tip constructed from a number of planes. The linewidth profile increases with increasing number of planes. However, the form of the profile itself is not affected allowing a qualitative interpretation of the line profiles defined by the Bloch and Néel wall contributions. It should be mentioned that a direct influence of the MFM tip on the magnetization distribution of the wall and vice versa has been neglected to a first approximation in the calculation. This is justified by the fact that no significant distortion of the asymmetry of the line profiles could be evidenced in the experiment.

In summary, from all measurements performed [including the as-grown virgin state, the state of perpendicular remanence (Fig. 2) and the state of perpendicular demagnetization (Fig. 3 below)], it is concluded that upon decreasing the film thickness from 100 to 20 nm an asymmetric Bloch wall transforms into an asymmetric Néel wall without formation of a cross-tie wall.

For the asymmetric Bloch wall, four energetically equivalent chiralities of the C shape exist which are shown schematically in Fig. 3(b). They are distinguished by the polarity of the Bloch wall (up or down) and by the Néel cap

rotation sense (clockwise or counterclockwise). For a 50-nm-thick film, the contrast is dominated by the Bloch core. An inversion of the Bloch orientation inverts the contrast, e.g., from black to white. Similarly, an inversion of the Néel cap rotation sense changes the asymmetry of the profile (the white border moves from one side to the other). It is observed that a single chirality for a single wall is induced after saturation in a field applied perpendicular to the film plane. This gives the Bloch wall a preferential orientation along the saturation field direction. In contrast, after perpendicular demagnetization, both Bloch orientations can be induced in a single wall. This gives rise in the MFM images to an alternating sequence of black and white segments as shown in Figs. 3(a) and 3(c). In addition, it is observed that the switch of the Bloch orientation is accompanied by a switch of the Néel cap rotation sense. In this way the magnetization of the Néel caps and the domains will maintain a flux closure structure. This switch of the Néel cap winding sense, coupled to the switch of the Bloch orientation, allows only two chiralities to be present along a single wall. This is clearly evidenced by the MFM line scans across the black and white segments [Figs. 3(c) and 3(d)] on a 50-nm-thick film. The reversal of the Bloch part from black to white is accompanied by a reversal of the Néel cap asymmetry. A consequence is that Bloch lines exist separating the different segments of opposing Bloch wall orientation.

In conclusion, we have evidenced the transformation of an asymmetric Bloch wall into an asymmetric Néel wall in epitaxial Co films characterized by a moderate  $Q$  factor. This transition occurs in a particularly thin thickness region (20 nm) without formation of cross-tie walls. It is furthermore shown that only two wall chiralities are stabilized along a single wall.

The authors wish to thank J. Arabski for technical support with the MBE growth of the samples. This work was partly supported by the EC-TMR program "Dynaspin" No. FMRX-CT97-0124 and the EC program "Magneis" No. IST-1999-11433.

<sup>1</sup>A. E. LaBonte, J. Appl. Phys. **40**, 2450 (1969).

<sup>2</sup>R. Scheinfein, J. Unguris, J. L. Blue, K. J. Coakley, D. T. Pierce, and J. Celotta, Phys. Rev. B **43**, 3395 (1991).

<sup>3</sup>A. Aharoni and J. P. Jakubovics, Phys. Rev. B **43**, 1290 (1991).

<sup>4</sup>A. Hubert and R. Schäfer, *Magnetic Domains* (Springer, Berlin, 1998), p. 153.

<sup>5</sup>M. Löhndorf, A. Wadas, H. A. M. van der Berg, and R. Wiensendanger, Appl. Phys. Lett. **68**, 3635 (1996).

<sup>6</sup>H.-N. Lin, Y. H. Chiou, B.-M. Chen, H.-P. D. Shieh, and C.-R. Chang, J. Appl. Phys. **83**, 4997 (1998).

<sup>7</sup>E. Zueco, W. Rave, R. Schäfer, M. Mertig, and L. Schultz, J. Magn. Mater. **196-197**, 115 (1999).

<sup>8</sup>W. Rave and A. Hubert, J. Magn. Mater. **184**, 179 (1998).

<sup>9</sup>I. L. Prejbeanu, J. Arabski, L. D. Buda, and K. Ounadjela (unpublished).

<sup>10</sup>M. R. Scheinfein and J. L. Blue, J. Appl. Phys. **69**, 7740 (1991).

<sup>11</sup>A. Aharoni and J. P. Jakubovics, Appl. Phys. Lett. **59**, 369 (1991).

<sup>12</sup>The modeled tip has a pyramidal shape constructed from magnetic cubes with uniform magnetization only on the pyramide surface layer and non-magnetic cubes inside the pyramide. The cell parameter is 2 nm.

<sup>13</sup>R. B. Proksch, T. E. Schäfer, B. M. Moskowitz, E. D. Dahlberg, D. A. Bazylinski, and R. B. Frankel, Appl. Phys. Lett. **66**, 2582 (1995).